



## Facile chemical activation process of kapok husk as a low-cost biosorbent for removal methylene blue dye in aqueous solution

RAHMIANA ZEIN<sup>1\*</sup>, HAMDHAN FATHONY<sup>1</sup>, PUTRI RAMADHANI<sup>2</sup>  
and DESWATI DESWATI<sup>3</sup>

<sup>1</sup>Laboratory of Environmental Analytical Chemistry, Department of Chemistry, Andalas University, Padang 25163, Indonesia, <sup>2</sup>Research Center for Chemistry, National Research and Innovation Agency of Indonesia, Jakarta 10340, Indonesia and <sup>3</sup>Laboratory of Applied Analytical Chemistry, Department of Chemistry, Andalas University, Padang 25163, Indonesia

(Received 3 March, revised 19 May, accepted 29 October 2023)

**Abstract:** This study discusses kapok husk (KH) activated by  $\text{HNO}_3$  as a biosorbent for methylene blue dye and analyses its adsorption ability. The adsorption capacity of KH is  $330.161 \text{ mg g}^{-1}$  with optimum conditions at pH 9, concentration  $5500 \text{ mg L}^{-1}$ , contact time 15 min, and biosorbent temperature  $25^\circ\text{C}$ . The isotherm study followed the Langmuir isotherm model, as seen from the  $R^2$  value of 0.9993 and maximum adsorption capacity of  $312.5 \text{ mg g}^{-1}$ , which indicated a monolayer in the adsorption process. The kinetic data show that KH followed the pseudo-second-order model. The results of the TGA analysis show that thermal stability affects the performance of biosorbents in the adsorption process. FTIR and SEM-EDS characterisation results showed that electrostatic interactions, cation exchange, and pore filling regulate the methylene blue dye adsorption mechanism on the surface of the KH. The reusability of KH through adsorption–desorption cycle analysis was achieved five times. This indicates that the biosorbent can be economically feasible for real wastewater treatment based on its good reusability and simple preparation and activation.

**Keywords:** adsorption; isotherm; kinetics; kapok husk; methylene blue.

### INTRODUCTION

The textile industry has grown rapidly, accounting for two-thirds of the total dyestuff market. About 5–15 % of the dye is released into the wastewater during the dyeing process.<sup>1,2</sup> Water availability for various needs tends to decrease quantitatively and qualitatively. On the other hand, water demand tends to increase, so water resource management problems always arise. If the liquid waste is discharged into water bodies, it can harm human health.<sup>3,4</sup> The growth of toxic

\* Corresponding author. E-mail: rzein@sci.unand.ac.id  
<https://doi.org/10.2298/JSC230303084Z>

waste metal contamination in the environment was caused by increasing industrial activities and human lifestyle.<sup>5</sup> Synthetic dyes often used in industry were derivatives of indigo, anthraquinone, sulfur, triphenylmethyl (trityl) and azo. However, most synthetic dyes currently used in the industry were azo derivatives.<sup>1</sup> Methylene blue (MB) is one of the dyes used in the industry. MB can cause eye burns that result in permanent eye injury in humans and aquatic animals. MB can also cause gastrointestinal irritation with nausea, vomiting, diarrhoea, and skin irritation symptoms.<sup>6</sup>

One alternative that researchers widely use for dye wastewater treatment is the adsorption method. Nowadays, the researcher is concerned with producing low-cost adsorbents as an alternative material, such as using organic solid waste from agricultural and fishery by-products.<sup>4</sup> Several adsorbents have been reported for MB dye removals, such as bivalve shells ( $1 \text{ mg g}^{-1}$ )<sup>7</sup>, lala clam shells ( $9.615 \text{ mg g}^{-1}$ )<sup>8</sup>, catappa shells ( $88.620 \text{ mg g}^{-1}$ )<sup>9</sup>, lemongrass leaves ( $43.160 \text{ mg g}^{-1}$ )<sup>10</sup> and activated carbon from starch ( $38.314 \text{ mg g}^{-1}$ ).<sup>11</sup> The modification and carbonization process which requires high costs but has a lower adsorption capacity, is a consideration for researchers, so it is necessary to find an efficient, low-cost, abundant and environmentally friendly adsorbent. This research used chemically activated kapok waste to remove methylene blue dye.

Kapok (*Ceiba pentandra* L.) is a plant found in tropical forests in Indonesia. This plant is cultivated to use fibres as a filling material for pillows, mattresses, cushions, etc. Using kapok produces waste or by-products in the form of husk, which is usually thrown into the environment or burned, harming the environment. This kapok husk contains carbohydrates, and lignin has an active side that can absorb cationic pollutants.<sup>12</sup>

Previous research has been reported on using kapok husk to remove Pb(II) and Cd(II) ions with adsorption capacity of  $223.72$  and  $88.70 \text{ mg g}^{-1}$ , respectively.<sup>13</sup> Meanwhile, the adsorption of dyes using kapok peel has never been done before, so kapok husk was investigated as an MB adsorbent with the batch method by taking into account the parameters of pH, concentration, contact time and heating temperature of the biosorbent. The isotherm analysis, kinetic analysis, and characterization of biosorbent were studied in order to determine the adsorption mechanism of MB dye on kapok husk.

## EXPERIMENTAL

### Materials and methods

Kapok husk (*Ceiba pentandra* L.) samples were collected from the Ombilin kapok plantation in West Sumatera, Indonesia. Methylene blue, HNO<sub>3</sub>, NaOH, buffer solution and acetic acid were purchased from Merck. Methylene blue dye was diluted with double-distilled water to make a stock solution. The pH of the solution was adjusted using NaOH (0.01 M) and HNO<sub>3</sub> (0.01 M). The initial and final concentration of the solution was measured using a UV–Vis spectrophotometer (Genesys 20 Thermo Scientific).

### *Preparation and activation of Kapok husk biosorbent*

The kapok husk was cleaned and dried, cut into small pieces, and ground using a grinder. Then, the size was uniformed using a 400 mesh sieve ( $\leq 36 \mu\text{m}$ ) to form a powder.<sup>13</sup> The kapok husk powder was soaked for 3 h in 0.01 M  $\text{HNO}_3$  with a ratio of powder to  $\text{HNO}_3$  of 1:3.<sup>14</sup> After that, it was washed with distilled water until the pH was neutral, filtered and air-dried.<sup>13,15</sup>  $\text{pH}_{\text{pzc}}$  was determined by adding 0.1 g of kapok peel powder into 25 mL of 0.1 M KCl solution at pH 2–9, then stirring for 24 h. Then, the initial pH versus  $\Delta\text{pH}$  (final pH–initial pH) was plotted and the point of intersection at  $y = 0$  was obtained.<sup>9,13</sup>

### *Biosorbent characterization*

The biosorbents were characterized by Fourier transform infra-red spectroscopy (FTIR), scanning electron microscope with energy dispersive spectroscopy (SEM-EDS), X-ray fluorescence (XRF) and thermogravimetric analysis (TGA). FTIR (IRTracer-100-Shimadzu) analysed the kapok husk's functional groups before and after dye adsorption. SEM-EDS (Inspect F50) was used to analyse the surface morphology of kapok husk before and after dye adsorption. XRF (PANalytical Epsilon 3) was used to determine the chemical composition of kapok husk before and after dye adsorption. TGA (Shimadzu DTG-60) was used to observe changes in mass with a function of time and temperature.

### *Biosorption studies*

Using a batch system, the adsorption process was investigated. Batch studies were carried out at various pH (5–10), initial MB dye concentration (300–6000 mg L<sup>-1</sup>), contact time (5–60 min) and biosorbent temperature (25, 50, 75 and 100 °C), with 10 ml of dye solution, biosorbent mass 0.1 g, and stirring speed 150 rpm. The mixture was filtered and analysed by UV-Vis spectrophotometer at 664 nm. The amount of MB dye adsorbed into the adsorbent was calculated by the following equation:

$$q_e = \frac{V(C_0 - C_e)}{m} \quad (1)$$

where  $C_0$ : initial dye concentration (mg L<sup>-1</sup>);  $C_e$ : concentration of dye at equilibrium (mg L<sup>-1</sup>);  $V$ : volume of solution (L);  $m$ : amount of biomass (g).<sup>16</sup>

## RESULTS AND DISCUSSION

### *Biosorbent characterization*

*Characterization of biosorbent using FTIR.* Functional groups on the kapok husk surface (KH) were identified by FTIR spectral analysis. The FTIR spectrum of the KH before and after MB dye adsorption is shown in Fig. 1. FTIR analysis was carried out from wave numbers 400–4000 cm<sup>-1</sup>, which can be seen in Fig. 1.

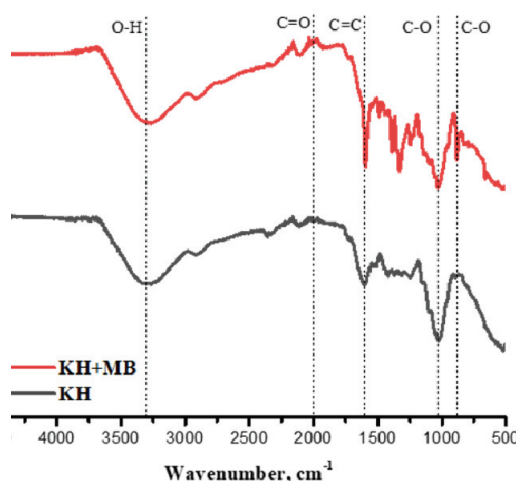


Fig. 1. FTIR spectrum of KH before and after MB dye adsorption.

Fig. 1 shows a peak at wave number  $3294.49\text{ cm}^{-1}$  before adsorption, indicating the presence of O–H stretching alcohol or intermolecular hydrogen bonds of carbohydrates in organic compounds (such as cellulose, hemicellulose and lignin). This wave figure shifted to  $3284.77\text{ cm}^{-1}$  after KH adsorbed MB. This shift suggested the formation of bonds between the MB dye and the hydroxyl group ( $-\text{OH}$ ) of the biosorbent.<sup>14</sup> The peak at  $896.86\text{ cm}^{-1}$  was shifted to  $883.40\text{ cm}^{-1}$ , indicating that the C–O bending group (alkene) contributed to the adsorption process. The wave number shift also occurred in the functional groups O–H alcohol ( $1369.96\text{ cm}^{-1}$ ) and O–H carboxylic acids ( $1417.68\text{ cm}^{-1}$ ). Oxygen-containing functional groups such as alcohols and carboxylic acids could bind to methylene blue molecules.<sup>17</sup> The shift in the wave number to either a larger or a smaller number indicates a change in the vibrational energy and a change in the inter and intra-molecular bonds in the biosorbent structure, as well as an interaction between the biosorbent functional group and MB dye in the form of electrostatic interactions.<sup>18</sup> The presence of MB molecules on the surface of the biosorbent was proved by the shift of the C–N group of aromatic amines from  $1244.09$  to  $1246.02\text{ cm}^{-1}$ . A heterocyclic amine and an amine group linked to an aromatic ring make up the dye MB.<sup>10</sup>

*Characterization of biosorbent using SEM-EDS.* SEM-EDS analysis provides information on the surface morphology and chemical composition of the biosorbent. The electrons from the high-energy beam used during SEM analysis interact with the atoms of the material's surface matrix, producing various types of signals containing information about the sample's surface morphology and the results are obtained in photographs.<sup>19</sup> SEM testing can also provide qualitative

information regarding the distribution pattern of methylene blue dye on the surface of the biosorbent.<sup>20</sup> The sample testing results using SEM can be seen in Fig. 2.

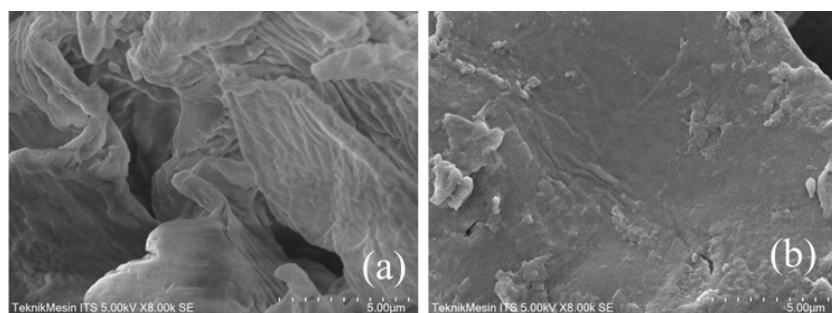


Fig. 2. SEM photos of kapok husk (a) before and (b) after adsorption.

Fig. 2 (a and b) shows the surface of the biosorbent before and after the adsorption of methylene blue at a magnification of 8000 times. In Fig. 2a, it can be seen that the surface of the biosorbent before the adsorption of the dye has a rough surface and has large cavities and pores. Based on the size of the hole and pores, it can be assumed that the holes and pores in the biosorbent most likely play a role in the adsorption of methylene blue dye. Fig 2b confirms that cavities and pores play a role in the adsorption of methylene blue dye, where the surface of the biosorbent, after adsorption MB, becomes smoother due to the trapping of methylene blue dye molecules and covers the cavities and pores of the biosorbent. This indicates that the process of adsorbing methylene blue dyes, apart from occurring chemically due to the abundance of functional groups on the surface, also occurs physically through the pores on the surface of the biosorbent.<sup>21</sup> The same result was reported by Mosoarca *et al.*<sup>22</sup>

In addition to qualitatively analysing the surface morphology of the biosorbent, SEM-EDS can also explore the abundance of elements present on the surface of the biosorbent and prove the adsorption of methylene blue dye on the surface of the biosorbent and confirmed by the results of the EDS analysis. Table I displays the EDS analysis outcomes of biosorbents before and after adsorption.

TABLE I. The relative abundance of elements (%) on the surface of the biosorbent (KH) before and after MB adsorption

Element	Before adsorption	After adsorption
C	27.78	35.55
O	61.96	51.69
Si	0.90	0.68
S	3.28	9.42
Ca	6.08	2.67

Based on Table I, elements O and C were more dominant than other elements. The biosorbent was an organic compound rich in C and O atoms. The biosorbent's increase in the percentage of C and S elements demonstrates that it successfully adsorbed the methylene blue dye.<sup>23</sup> Due to the presence of these elements throughout the adsorption process, the percentage of O, Si and Ca elements decreased following the adsorption of the methylene blue dye. The same result has been reported by Zein *et al.*,<sup>10</sup> where lemongrass leaves biowaste in the EDS analysis for elements C and S showed an increase in the percentage of elements, while elements O, Si, and Ca showed a decrease in the percentage of elements due to the formation of various interactions between dyes and biosorbents during adsorption process.

*Characterization of biosorbent using XRF.* XRF analysis provides information on the chemical composition of kapok husk before and after dye adsorption.<sup>24</sup> XRF analysis was also associated with EDS analysis. XRF analysis can be seen in Table II.

TABLE II. Chemical composition (%) of kapok husk before and after MB dye adsorption

Element/Oxide	KH	KH + MB
K	11.026	0.24
K <sub>2</sub> O	9.652	0.117
S	3.452	62.932
SO <sub>3</sub>	7.035	76.525
Si	1.222	0.534
SiO <sub>2</sub>	2.038	1.15

Table II shows that the dominant KH contains K and K<sub>2</sub>O, where the percentage of K and K<sub>2</sub>O was above 9 %. It can be seen that the adsorption of methylene blue on the KH biosorbent significantly reduces of the K element. The K element decreased from 11.026 to 0.24 %, indicating that the site occupied by both K elements was replaced by methylene blue during the adsorption process, indicating the occurrence of cation exchange.<sup>24,25</sup> Element S in KH biosorbent increased significantly from 3.452 to 63.932 %, indicating that both biosorbents have adsorbed methylene blue.<sup>9</sup>

*Characterization of biosorbent using TGA.* TGA analysis aims to determine the mass fraction and stability of the biosorbent against high-temperature treatment.<sup>10,21</sup> The biosorbent thermogram can be seen in Fig. 3.

The results of TGA analysis on kapok husk showed a degradation step, as shown in Fig. 3. The first stage at a temperature of 25 to 100 °C decreased the initial mass due to the loss of water molecules and volatile compounds on the surface of the biosorbent, so that the pores of the biosorbent were wide open.<sup>18</sup> In the second stage, at a temperature of 100–350 °C, the biosorbent decomposes at temperatures above 200 °C for the structural units of cellulose, hemicellulose and

lignin, which form  $\text{CO}_2$  gas and water.<sup>26,27</sup> At this stage, the destruction of all functional groups causes the adsorption capacity to be lower. In the third stage ( $>350\text{ }^\circ\text{C}$ ), the decomposition of biosorbent solid residues forms ash.<sup>10</sup>

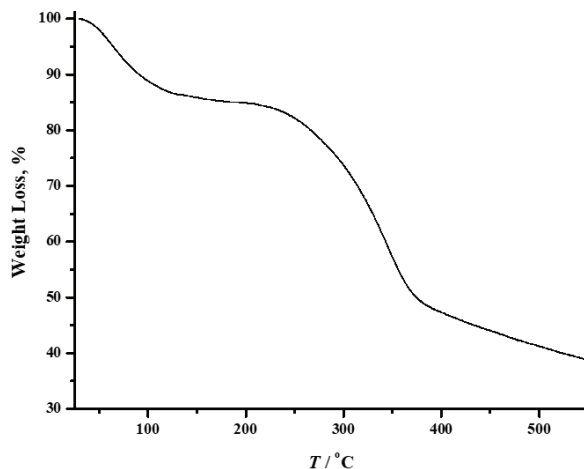


Fig. 3. Thermogram of kapok husk.

#### *Analysis of $pH_{\text{pzc}}$*

$pH_{\text{pzc}}$  was a pH value indicating that a solid's surface has a zero charge.  $pH_{\text{pzc}}$  was used to measure or determine the electrokinetic properties of a surface.<sup>28</sup> The pH value describes the point of zero charges only for systems where  $\text{H}^+/\text{OH}^-$  was the potential determining ion. Due to the presence of functional groups such as  $\text{OH}^-$  groups, the adsorption of cationic dyes was favoured at  $\text{pH} > pH_{\text{pzc}}$ .<sup>29</sup> In contrast, adsorption of anionic dyes was favoured at  $\text{pH} < pH_{\text{pzc}}$ , where the surface becomes positively charged.<sup>30</sup>

In this study,  $pH_{\text{pzc}}$  was used to detect the zero charge of kapok husk. Fig. 4 shows that the  $pH_{\text{pzc}}$  of kapok husk was 7.3. This proves that the zero charge on the kapok husk was at pH 7.3. The removal process of cationic dyes in aqueous solutions using kapok husk at a pH above 7.3. Meanwhile, a pH value lower than 7.3 was not favourable for the adsorption of cationic dyes.

#### *Effect of pH*

Changes in pH solution have a strong influence on the adsorption process. The adsorption capacity of methylene blue dye by the kapok husk biosorbent increased until it reached the optimum solution pH at pH 9. The effect of this pH could be explained by the  $pH_{\text{pzc}}$  of the kapok husk, which was 7.3. At values higher than  $pH_{\text{pzc}}$ , the kapok husk particles acquire a negative surface charge, which leads to a stronger electrostatic attraction, making them suitable for adsorption of the cationic dye methylene blue.<sup>31</sup> Zein *et al.* also reported that the

optimum pH for MB adsorption using lemongrass leaves biowaste was pH 9.<sup>10</sup> The effect of pH on the adsorption capacity was shown in Fig 5.

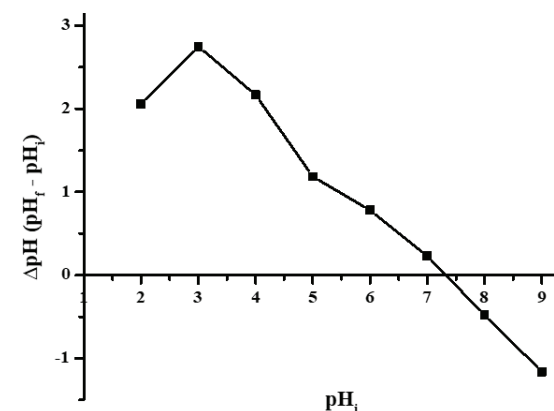


Fig. 4. pH<sub>pzc</sub> for kapok husk.

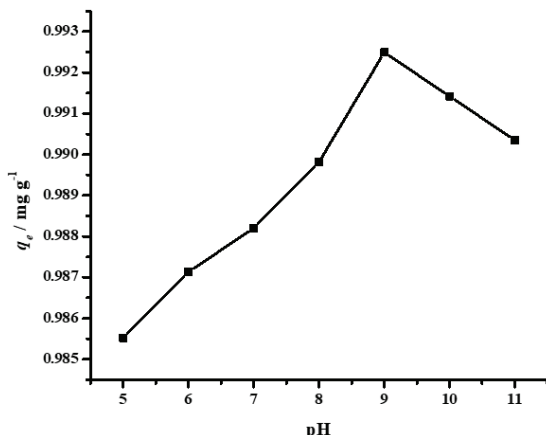


Fig. 5. Effect of the pH on methylene blue dye adsorption capacity. Experimental conditions: C<sub>0</sub>: 10 mg L<sup>-1</sup>; biosorbent mass: 0.1 g; stirring speed: 150 rpm; contact time: 60 min; particle size :  $\leq$ 36  $\mu$ m; MB volume: 10 mL.

#### Effect of initial concentration

The initial concentration of the dye affects the adsorption capacity value and shows the mechanism that occurs during the adsorption process. The MB dye concentration used to study KH adsorption capacity was 300–6000 mg L<sup>-1</sup> with an optimum pH of 9. Fig. 6 shows the adsorption capacity value increased from 300 mg L<sup>-1</sup> to a concentration of 5500 mg L<sup>-1</sup> with a capacity of adsorption of 314.08 mg g<sup>-1</sup>. Meanwhile, at a concentration higher than 5500 mg L<sup>-1</sup>, the adsorption capacity value decreased to 306.70 mg g<sup>-1</sup> at 6000 mg L<sup>-1</sup>. It can be assumed that the optimal adsorption capacity of KH was 314.08 mg g<sup>-1</sup> at a concentration of 5500 mg L<sup>-1</sup>.

The driving force or mobility of the dye molecules to diffuse will rise with an increase in the initial concentration of MB. As a result, mass was transferred

from the liquid phase (the dye solution) to the solid phase (the biosorbent), increasing the adsorption capacity. If it is supposed the MB concentration increases higher than the optimal adsorption capacity,<sup>10</sup> it will interfere with the interaction between KH and MB during the adsorption process so that the adsorption capacity decreases.<sup>9</sup>

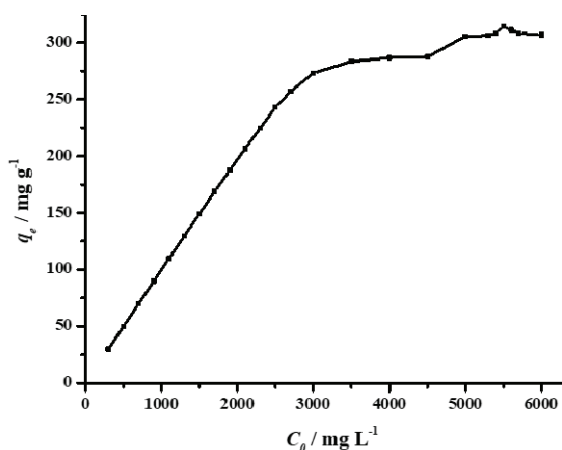


Fig. 6. Effect of the initial concentration on methylene blue dye adsorption capacity. Experimental conditions: pH: 9; biosorbent mass: 0.1 g; stirring speed: 150 rpm; contact time: 60 min; particle size:  $\leq 36 \mu\text{m}$ ; MB volume: 10 mL.

#### *Effect of contact time*

The influence of contact time on the biosorption process was conducted within 5, 15, 30, 45 and 60 min. The effect of contact time on the value of the adsorption capacity of KH can be seen in Fig 7. Fig 7 shows the adsorption capacity increased with the contact time from 5 to 15 min with an adsorption capacity value of  $330.16 \text{ mg g}^{-1}$ . However, after 15 min, the adsorption capacity decreased. In this study, it was assumed that the optimum contact time and equilibrium were reached within 15 min with the optimum adsorption capacity of  $330.16 \text{ mg g}^{-1}$ . Numerous positively charged adsorbent surfaces were readily available, which speeds up the adsorption process on KH. The adsorption process moves slowly because the active site of KH has been saturated after 15 min, and there was a repulsive interaction between MB and KH molecules.<sup>32</sup> The similar contact time results on cationic dye adsorption were observed using Terminalia catappa<sup>9</sup> and Lemongrass leaves biowaste.<sup>10</sup>

#### *Effect of biosorbent temperature*

The study of the temperature dependence of the sorption reaction provides valuable information about the enthalpy changes during adsorption. In addition, temperature changes will make the equilibrium capacity of the adsorbent different for a particular adsorbate.<sup>33</sup> Because many wastes containing different dyes were produced and disposed of at relatively high temperatures.<sup>34</sup> Therefore, to

determine the effect of heating temperature, the adsorption experiments were carried out at 25, 50, 75, and 100 °C, respectively, as shown in Fig. 8.

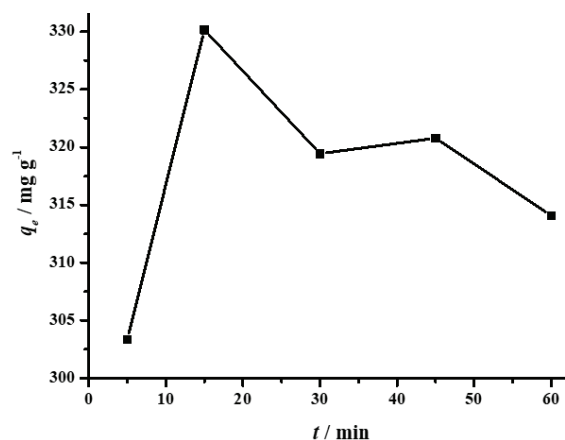


Fig. 7. Effect of the contact time on methylene blue dye adsorption capacity. Experimental conditions: pH: 9;  $C_0$ : 5500 mg L<sup>-1</sup>; biosorbent mass: 0.1 g; stirring speed: 150 rpm; particle size: ≤36 µm; MB volume: 10 mL.

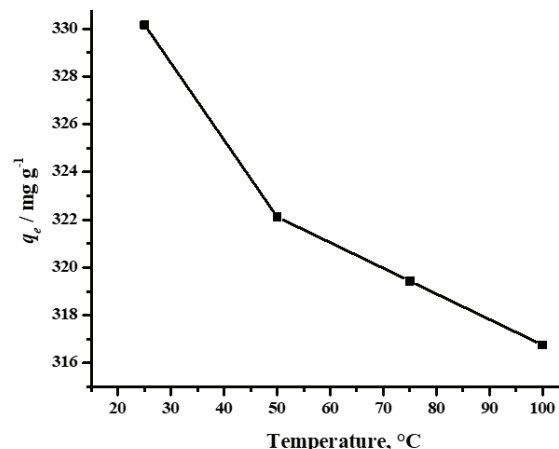


Fig. 8. Effect of the biosorbent temperature on methylene blue dye adsorption capacity. Experimental conditions: pH: 9;  $C_0$ : 5500 mg L<sup>-1</sup>; biosorbent mass: 0.1 g; stirring speed: 150 rpm; contact time: 15 min; particle size: ≤36 µm; MB volume: 10 mL.

Fig. 8 shows the effect of the biosorbent's heating temperature for KH was achieved at 25 °C with an adsorption capacity of 330.16 mg g<sup>-1</sup>. After the temperature was above 25 °C, the adsorption capacity decreased. This was due to damage to the biosorbent. Zein also reported the same thing for lemongrass leaves biowaste biosorbent, where the heating temperature of the biosorbent was reached at 25 °C.<sup>10</sup>

#### *Equilibrium isotherm modelling*

The adsorption isotherm model can describe the interaction between the adsorbent and adsorbate, which is an important factor in optimizing the use of the adsorbent<sup>35</sup> and the results can be seen in Fig. 9.

Based on Fig. 9, it can be seen that the  $R^2$  value in the Langmuir isotherm model was 0.9993 for KH. The value of  $R^2$ , which was close to 1, indicates that the adsorption process follows the Langmuir isotherm model. The Langmuir isotherm applies to the adsorption of a solute from a liquid solution when it corresponds to the adsorption of a single layer (monolayer) on the surface.<sup>36</sup> The value of each parameter of the adsorption isotherm model was used to predict the adsorption mechanism during the process and represented in Table III.

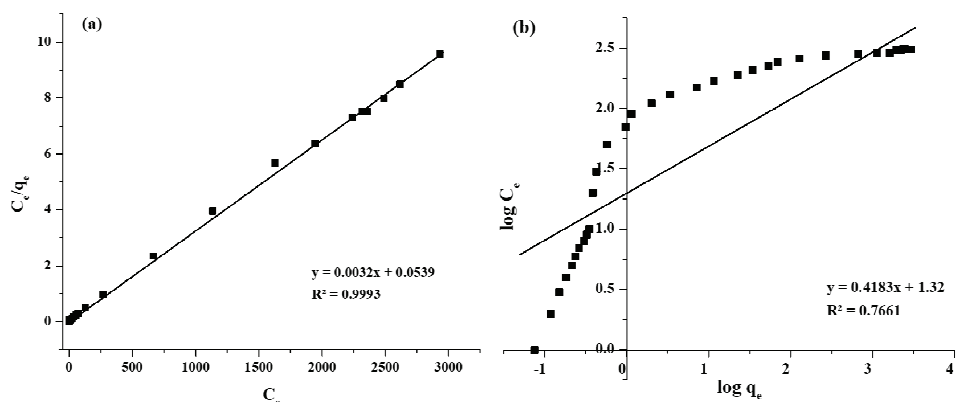


Fig. 9. Linear plots of: a) Freundlich isotherm and b) Langmuir for adsorption methylene blue dye by kapok husk.

Table III. Parameters of the adsorption isotherm model for adsorption MB dye by KH

Isotherm model	Constant	Value
Langmuir	$q_m / \text{mg g}^{-1}$	312.5000
	$K_L / \text{L mg}^{-1}$	0.0594
	$R^2$	0.9993
	$R_L$	0.0028–0.6275
	$K_F$	20.8929
	$1/n$	0.41835
Freundlich	$R^2$	0.7661

#### Kinetics modelling

In order to increase adsorption effectiveness and process scale factor, the kinetic model's definition of the adsorption mechanism has been helpful.<sup>37</sup> The physical and chemical characteristics of the adsorbent and the mass transmission method were crucial factors to consider when determining the adsorption mechanism.<sup>9</sup> The curve for pseudo-first-order, pseudo-second-order and intra-particle diffusion models to the contact time data were represented in Fig. 10 (a–c). As shown in Fig. 10a, a pseudo-first-order model allowed researchers to study the adsorption mechanism. The values of  $k_1$  and  $q_e$  were determined from the intercept and slope of the plot of  $\ln (q_e - q_t)$  versus  $t$  curve ( $y = 0.0122x + 1.7576$ ,

$R^2 = 0.046$ ). As observed in Fig. 10b, the  $k_2$  and  $q_e$  for the pseudo-second-order model were determined from the intercept and slope of the  $t/q_t$  versus  $t$  curve ( $y = 0.0032x - 0.001$ ,  $R^2 = 0.9995$ ). As shown in Fig. 10c, the intercept and slope of the  $t^{1/2}$  versus  $q_t$  plot ( $y = 0.0566x - 12.771$ ,  $R^2 = 0.064$ ) will give information about  $K_{\text{diff}}$  and  $C$  value.<sup>38</sup>

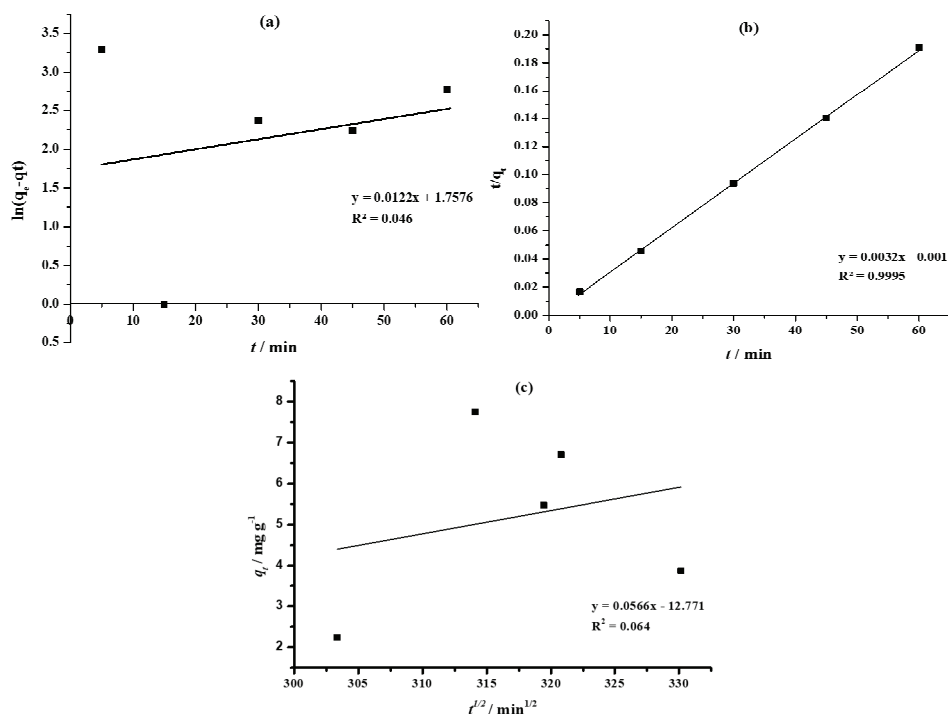


Fig. 10. Kinetic plots of: a) pseudo-first-order, b) pseudo-second-order and c) intra-particle diffusion for adsorption methylene blue dye by kapok husk.

The  $k_1$  and  $k_2$  were obtained with value  $-0.0122$  and  $0.0102 \text{ min}^{-1}$ , respectively. The correlation coefficient value ( $R^2$ ) obtained from pseudo-second-order kinetics (0.9995) was higher than the value from pseudo-first-order (0.046) and intra-particle diffusion (0.064). The lower value of  $R^2$  from pseudo-first order and intra-particle diffusion models indicated that the MB dye adsorption does not occur through diffusion and multilayer formation. The pseudo-second-order kinetics can adequately describe the adsorption of methylene blue by KH by chemisorption (chemical interaction).<sup>9</sup>

#### Adsorption-desorption analysis

The adsorption-desorption analysis was an important parameter to evaluate the regeneration/reusability of a biosorbent so that it can be estimated on a large

scale.<sup>4</sup> Reusability study was analysed by immersing the biosorbent using a desorbing agent. The desorption agent selected must be effective, environmentally friendly, and low-cost. One of the methylene blue desorption agents reported and effectively used was 30 % acetic acid.<sup>9</sup> 30 % acetic acid as a desorption agent causes electrostatic repulsion between methylene blue and the surface of the biosorbent so that methylene blue is released from the surface of the adsorbent.<sup>39</sup> The adsorption–desorption cycle for the KH biosorbent can be seen in Fig. 11.

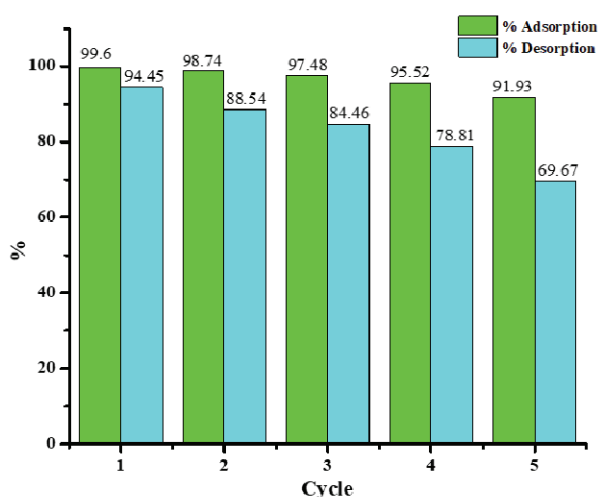


Fig. 11. Adsorption-desorption cycle of methylene blue dye onto kapok husk.

Fig. 11 shows the reusability of the biosorbent, which was reused for five cycles. The adsorption percentage decreased from the first (99.6 %) to the fifth (91.93 %) cycle. Zein *et al.* revealed that the active site on the surface of the biosorbent was saturated with methylene blue molecules, which was why the adsorption percentage declined with increasing cycles. Extreme pH circumstances trigger the degradation of biosorbent, which also exhibits blocked pores and active sites on its surface.<sup>10</sup>

#### Biosorption mechanism

The mechanism of biosorption was important to determine, which can predict how the mechanism of adsorption occurs from the data obtained. The biosorption mechanism can be predicted using the results of the influence of optimum conditions, adsorption isotherm studies, adsorption kinetics studies and biosorbent characterization using FTIR and SEM-EDS.<sup>9,10</sup> The adsorption mechanism can be made based on the above explanation. This is represented in Fig. 12.

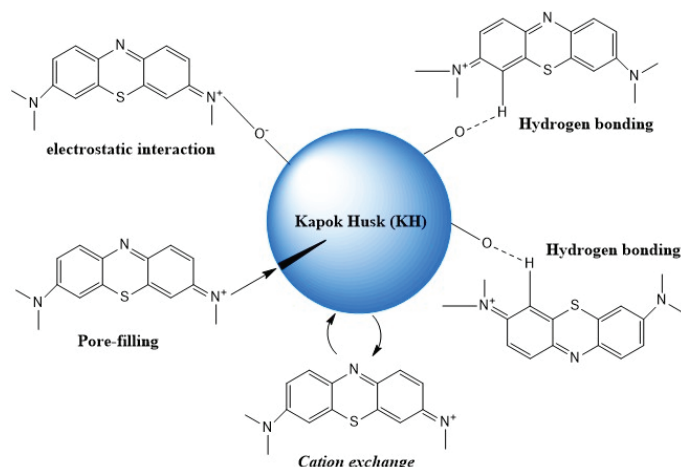


Fig. 12. Adsorption mechanism prediction of removal methylene blue dye onto kapok husk.

Based on Fig. 12, the adsorption mechanism between adsorbent and adsorbate was obtained from the data of  $pH_{pzc}$  biosorbent KH ( $pH_{pzc} 7.3$ ), and the positive and negative charges on the surface of the biosorbent will be the same. For the adsorption of cationic dyes, the pH value must be greater than  $pH_{pzc}$ . It was intended that the functional groups on the surface of the biosorbent were deprotonated so that it would make the surface of the biosorbent negatively charged.<sup>40</sup> At the same time, the methylene blue will be protonated so that cationic exchange and electrostatic interactions occur between cationic methylene blue and negatively charged KH biosorbent. The EDS and XRF analysis results showed the cation exchange during the adsorption of methylene blue dye on the surface of the biosorbent. SEM analysis showed the results on the surface of the biosorbent before and after adsorption. A smoother surface after adsorption occurs due to the filling of biosorbent pores by methylene blue dye.

The adsorption ability of methylene blue by KH biosorbent was compared with other biosorbents. This needs to be done to see how far the research progresses and how it is positioned among the advantages and disadvantages of other biosorbents. A comparison of KH biosorbent with other biosorbents can be seen in Table IV. Table IV shows that the KH adsorption capacity value is close to the adsorption capacity value of the activated carbon from agricultural solid waste.<sup>41,42</sup> This could indicate that chemically activated KH performs well with high adsorption capacity, low cost, and environmental friendliness.

#### *Application in real wastewater treatment*

This work investigated kapok husk's efficiency in the biosorption of methylene blue dye removal in wastewater. Due to other competitive species in real wastewater, performance was typically lower than in experiments.<sup>9</sup> The waste-

water used in this study was sourced from the Environmental Chemistry Laboratory, Andalas University. Table V shows the results of applying the optimum conditions for MB adsorption in wastewater.

TABLE IV. Ability of kapok husk adsorbent for removal methylene blue dye in comparison to other adsorbents

No	Biosorbent	$q_m / \text{mg g}^{-1}$	Reference
1	Kapok husk	330.16	This study
2	Activated carbon from tea seed shells	324.70	42
3	Activated carbon derived from lignocellulosic agriculture wastes	148.80	41
4	Walnut shells powder	178.90	43
5	Coconut leaf	112.35	44
6	Terminalia catappa	88.62	9
7	Lemongrass leaves biowaste	43.15	10
8	<i>Platanus orientalis</i> leaf powder	114.94	38
9	Carbon-coated magnetic nanocomposite	110.63	45
10	<i>Streptomyces fradiae</i> biomass	59.63	46

Table V. Removal performance of kapok husk on real wastewater

Waste code	pH	Biosorbent temperature, °C	$C_0 / \text{mg L}^{-1}$	$C_e / \text{mg L}^{-1}$	R / %
Real	7.245	25	1.8445	0.2627	85.76
Optimum	9	25	2.1341	0.1877	91.21

Table V shows that good % removal was achieved for the adsorption of methylene blue dye in wastewater at optimum pH for biosorbent. At the pH of the natural solution (without adjusting the pH), the percentage of removal (%) obtained was lower than by adjusting the pH first. This informs that KH can be an excellent biosorbent to remove MB dye in aqueous solutions. Biosorbent residues can be used in concrete mixes to remove adsorbents. Another safe disposal method can be the impregnation in polymer resins and other cement mixtures.<sup>9,15</sup>

#### CONCLUSION

The MB dye adsorption process using KH has good results. The adsorption capacity of KH was  $330.161 \text{ mg g}^{-1}$  with optimum conditions at pH 9, a concentration of  $5500 \text{ mg L}^{-1}$ , a contact time of 15 min, and a heating temperature of  $25^\circ\text{C}$ . The isotherm study followed the Langmuir isotherm model, as seen from the  $R^2$  value of 0.9993, which indicated a monolayer layer in the adsorption process. The kinetic data show that KH follows a pseudo-second-order kinetic model. The adsorption-desorption results showed that the biosorbent gave an adsorption–desorption cycle of five times; this indicates that the biosorbent can be economically feasible for real wastewater treatment based on its good reuse pot-

ential. Applying biosorbent to laboratory liquid waste and textile industry waste gives a high % removal result of above 90% at optimum biosorbent conditions.

*Acknowledgements.* We acknowledge the Directorate of Research, Technology and Community Service, Directorate General of Higher Education, Research and Technology, Ministry of Education, Culture, Research, and Technology (Grant Numbers 086/E5/PG.02.00.PT/2022, Fiscal Year 2022).

#### ИЗВОД

#### ОЛАКШАН ПРОЦЕС ХЕМИЈСКЕ АКТИВАЦИЈЕ КАПОК ЉУСКЕ КАО ЈЕФТИНОГ БИОСОРБЕНТА ЗА УКЛАЊАЊЕ МЕТИЛЕН ПЛАВЕ БОЈЕ У ВОДЕНОМ РАСТВОРУ

RAHMIANA ZEIN<sup>1</sup>, HAMDHAN FATHONY<sup>1</sup>, PUTRI RAMADHANI<sup>2</sup> и DESWATI<sup>3</sup>

<sup>1</sup>Laboratory of Environmental Analytical Chemistry, Department of Chemistry, Andalas University, Padang 25163, Indonesia, <sup>2</sup>Research Center for Chemistry, National Research and Innovation Agency of Indonesia, Jakarta 10340, Indonesia и <sup>3</sup>Laboratory of Applied Analytical Chemistry, Department of Chemistry, Andalas University, Padang 25163, Indonesia

Ова студија разматра капок љуску (КН) активирану помоћу  $\text{HNO}_3$ , као потенцијални биосорбент за метилен плаву боју (МВ), и анализира њену способност адсорпције. Капацитет адсорпције КН је  $330,161 \text{ mg g}^{-1}$  при оптималним условима: pH 9, концентрација  $5500 \text{ mg L}^{-1}$ , време контакта  $15 \text{ min}$  и температура биосорбента  $25^\circ\text{C}$ . Студија изотерме је пратила Ленгмиров модел, што се види из вредности  $R^2$  од 0,9993, и максималног капацитета адсорпције од  $312,5 \text{ mg g}^{-1}$ , што указује на монослој у процесу адсорпције. Кинетички подаци показују да КН следи модел псевдо-другог реда. Резултати TGA анализе показују да термичка стабилност утиче на перформансе биосорбената у процесу адсорпције. Резултати FTIR и SEM-EDS карактеризације су показали да електростатичке интеракције, размена катјона и попуњавање пора регулишу механизам адсорпције МВ на површини КН. Поновна употреба КН кроз циклус адсорпције–десорпције постигнута је пет пута. Биосорбент може бити економски исплатив за прави третман отпадних вода на основу могућности његове добре поновне употребе и једноставног начина припреме и активирања.

(Примљено 3. марта, ревидирано 19. маја, прихваћено 29. октобра 2023)

#### REFERENCES

1. G. Samchetshabam, A. Hussan, T. G. Choudhury, S. Gita, *Environ. Ecol.* **35** (2017) 2349 (<https://jurnal.fmipa.unila.ac.id/sains/article/view/205/pdf>)
2. S. Afrin, H. R. Shuvo, B. Sultana, F. Islam, A. A. Rus'd, S. Begum, M. N. Hossain, *Heliyon* **7** (2021) e08102 (<https://doi.org/10.1016/j.heliyon.2021.e08102>)
3. Safni, D. F. Wulandari, Zulfarman, Maizatisna, T. Sakai, *MIPA FMIPA Univer. Lampung* **14** (2008) 143 (<https://jurnal.fmipa.unila.ac.id/sains/article/view/205/pdf>)
4. P. Ramadhani, R. Zein, Z. Chaidir, L. Hevira, *J. Zarrah* **7** (2019) 46 (<https://doi.org/10.31629/zarah.v7i2.1396>)
5. Y. Rahmadani, F. Rozani, A. Rahmi, M. Suardi, *J. Katalisator* **2** (2017) 29
6. S. A. Umuren, U. J. Etim, A. U. Israel, *J. Mater. Environ. Sci.* **4** (2013) 75 (<https://www.jmaterenvironsci.com/Journal/vol4-1.html>)
7. K. Z. Elwakeel, A. M. Elgarahy, S. H. Mohammad, *J. Environ. Chem. Eng.* **5** (2017) 578 (<https://doi.org/10.1016/j.jece.2016.12.032>)

8. A. Alseddig, A. Eljedi, A. Kamari, in *Proc. Int. Conf. Educ. Math. Sci. 2016 Conjunction with 4th Int. Postgrad. Conf. Sci. Math. 2016* **040003** (2017) (<https://doi.org/10.1063/1.4983899>)
9. L. Hevira, Zilfa, Rahmayeni, J. O. Ighalo, H. Aziz, R. Zein, *J. Ind. Eng. Chem.* **97** (2021) 188 (<https://doi.org/10.1016/j.jiec.2021.01.028>)
10. R. Zein, J. S. Purnomo, P. Ramadhani, M. F. Alif, S. Safni, *Sep. Sci. Technol.* **57** (2022) 1 (<https://doi.org/10.1080/01496395.2022.2058549>)
11. F. Benhachem, T. Attar, F. Bouabdallah, *Chem. Rev. Lett.* **2** (2019) 33 (<https://doi.org/10.22034/crl.2019.87964>)
12. K. Hori, M. E. Flavier, S. Kuga, T. B. T. Lam, K. Iiyama, *J. Wood Sci.* **46** (2000) 401 (<https://doi.org/10.1007/BF00776404>)
13. R. Zein, D. Nofita, R. Refilda, H. Aziz, *Chim. Nat. Acta* **7** (2019) 37 (<https://doi.org/10.24198/cna.v7.n1.20813>)
14. L. Hevira, R. Zein, E. Munaf, *J. Katalisator* **4** (2019) 42
15. L. Hevira, Zilfa, Rahmayeni, J. O. Ighalo, R. Zein, *J. Environ. Chem. Eng.* **8** (2020) 104290 (<https://doi.org/10.1016/j.jece.2020.104290>)
16. R. Zein, M. Suciandica, *J. Katalisator* **7** (2022) 63 (<http://publikasi.lldikti10.id/index.php/katalisator/article/view/963>)
17. S. Sahu, S. Pahi, S. Tripathy, S. K. Singh, A. Behera, U. K. Sahu, R. K. Patel, *J. Mol. Liq.* **315** (2020) 113743 (<https://doi.org/10.1016/j.molliq.2020.113743>)
18. J. Ooi, L. Y. Lee, B. Y. Z. Hiew, S. Thangalazhy-Gopakumar, S. S. Lim, S. Gan, *Bioresour. Technol.* **245** (2017) 656 (<https://doi.org/10.1016/j.biortech.2017.08.153>)
19. L. Bulgarie, L. Belén, O. Solomon, M. Iqbal, J. Nisar, K. Adesina, F. Alakhras, M. Kornaros, I. Anastopoulos, *J. Mol. Liq.* **276** (2019) 728 (<https://doi.org/10.1016/j.molliq.2018.12.001>)
20. N. K. Gupta, A. Gupta, P. Ramteke, H. Sahoo, A. Sengupta, *J. Mol. Liq.* **274** (2019) 148 (<https://doi.org/10.1016/j.molliq.2018.10.134>)
21. R. Zein, Z. Chadir, S. Fauzia, P. Ramadhani, *J. Kim. Val.* **8** (2022) 10 (<https://doi.org/10.15408/jkv.v8i1.22566>)
22. G. Mosoarca, C. Vancea, S. Popa, M. Radulescu-Grad, S. Boran, *J. Serb. Chem. Soc.* **87** (2022) 39 (<https://doi.org/10.2298/jsc220316039m>)
23. D. Pathania, S. Sharma, P. Singh, *Arab. J. Chem.* **10** (2017) S1445 (<https://doi.org/10.1016/j.arabjc.2013.04.021>)
24. M. K. Dahri, M. R. R. Kooh, L. B. L. Lim, *Alexandria Eng. J.* **54** (2015) 1253 (<https://doi.org/10.1016/j.aej.2015.07.005>)
25. L. B. L. Lim, N. Priyantha, C. Hei Ing, M. Khairud Dahri, D. T. B. Tennakoon, T. Zehra, M. Suklueng, *Desalin. Water Treat.* **53** (2013) 964 (<https://doi.org/10.1080/19443994.2013.852136>)
26. L. Burhenne, J. Messmer, T. Aicher, M. Laborie, *J. Anal. Appl. Pyrolysis* **101** (2013) 177 (<https://doi.org/10.1016/j.jaap.2013.01.012>)
27. L. Hevira, Zilfa, Rahmayeni, J. O. Ighalo, H. Aziz, R. Zein, *J. Ind. Eng. Chem.* **97** (2021) 188 (<https://doi.org/10.1016/j.jiec.2021.01.028>)
28. W. Liu, C. Yao, M. Wang, J. Ji, L. Ying, C. Fu, *Environ. Prog. Sustain. Energy* **32** (2013) 655 (<https://doi.org/10.1002/ep.11680>)
29. I. Bencheikh, K. Azoulay, J. Mabrouki, S. El Hajjaji, A. Dahchour, A. Moufti, D. Dhiba, *Sci. Afr.* **9** (2020) (<https://doi.org/10.1016/j.sciaf.2020.e00509>)

30. M. T. Yagub, T. K. Sen, S. Afroze, & H. M. Ang, *Adv. Colloid Interface Sci.* **209** (2014) 172 (<https://doi.org/10.1016/j.cis.2014.04.002>)
31. W. Hassan, U. Farooq, M. Ahmad, M. Athar, M. A. Khan, *Arab. J. Chem.* **10** (2017) S1512 (<https://doi.org/10.1016/j.arabjc.2013.05.002>)
32. G. K. Cheruiyot, W. C. Wanyonyi, J. J. Kiplimo, E. N. Maina, *Sci. Afr.* **5** (2019) 1 (<https://doi.org/10.1016/j.sciaf.2019.e00116>)
33. J. Guo, B. Li, L. Liu, K. Lv, *Chemosphere* **111** (2014) 225 (<https://doi.org/10.1016/j.chemosphere.2014.03.118>)
34. M. M. Felista, W. C. Wanyonyi, G. Ongera, *Sci. Afr.* **7** (2020) e00283 (<https://doi.org/10.1016/j.sciaf.2020.e00283>)
35. P. Wang, Q. Ma, D. Hu, L. Wang, *Desalin. Water Treat.* **57** (2015) 10261 (<https://doi.org/10.1080/19443994.2015.1033651>)
36. M. A. Al-Ghouti, D. A. Da'ana, *J. Hazard. Mater.* **393** (2020) 122383 (<https://doi.org/10.1016/j.jhazmat.2020.122383>)
37. F. Batool, J. Akbar, S. Iqbal, S. Noreen, S. N. A. Bukhari, *Bioinorg. Chem. Appl.* **2018** (2018) (<https://doi.org/10.1155/2018/3463724>)
38. M. Peydayesh, A. Rahbar-kelishami, *J. Ind. Eng. Chem.* (2014) 1 (<https://doi.org/10.1016/j.jiec.2014.05.010>)
39. A. N. Labaran, Z. U. Zango, Z. N. Garba, A. Science, K. State, *Sci. World J.* **14** (2019) 66 (<https://www.ajol.info/index.php/swj/article/view/208624>)
40. M. Z. A. Zaimee, M. S. Sarjadi, M. L. Rahman, *Water (Switzerland)* **13** (2021) (<https://doi.org/10.3390/w13192659>)
41. H. M. El-Bery, M. Saleh, R. A. El-Gendy, M. R. Saleh, S. M. Thabet, *Sci. Rep.* **12** (2022) 1 (<https://doi.org/10.1038/s41598-022-09475-4>)
42. J. J. Gao, Y. B. Qin, T. Zhou, D. D. Cao, P. Xu, D. Hochstetter, Y. F. Wang, *J. Zhejiang Univ. Sci., B* **14** (2013) 650 (<https://doi.org/10.1631/jzus.B12a0225>)
43. Y. Miyah, A. Lahrichi, M. Idrissi, A. Khalil, F. Zerrouq, *Surfaces Interfaces* **11** (2018) 74 (<https://doi.org/10.1016/j.surfin.2018.03.006>)
44. A. H. Jawad, R. A. Rashid, R. M. A. Mahmuod, M. A. M. Ishak, N. N. Kasim, K. Ismail, *Desalin. Water Treat.* **57** (2016) 8839 (<https://doi.org/10.1080/19443994.2015.1026282>)
45. N. Nguyen, T. Q. Phan, C. T. Pham, H. Nguyen, S. Pham, Q. K. Nguyen, D. Ngunyen, *J. Serb. Chem. Soc.* **88** (2023) 423 (<https://doi.org/10.2298/JSC220802080N>)
46. Z. Y. Velkova, G. K. Kirova, M. S. Stoytcheva, V. K. Gochev, *J. Serb. Chem. Soc.* **83** (2018) 107 (<https://doi.org/10.2298/JSC170519093V>).